

Learning Social Circles in Ego Networks based on Multi-View Social Graphs

Chao Lan¹, Yuhao Yang², Xiaoli Li¹, Bo Luo¹ and Jun Huan¹

¹EECS Department, University of Kansas
Emails: {clan, xiaolili, bluo, jhuan}@ittc.ku.edu
²ZL Technologies, Inc
Email: yangyuhao05@gmail.com

June 15, 2022

Abstract

Automatic social circle detection in ego-networks is becoming a fundamentally important task for social network analysis, which can be used for privacy protection or interest group recommendation. So far, most studies focused on how to detect overlapping circles or how to perform detection using both network structure and its node profiles. This paper asks an orthogonal research question: how to detect social circles by leveraging the multiple views of the network structure? As a first step, we crawl ego networks from Twitter to construct multi-view social graphs with six views, including two relationship views, three interaction views and one content view. Then, we apply both standard and our modified multi-view spectral clustering methods on the graph to detect circles. Based on extensive automatic and manual evaluations, we deliver two major findings: first, multi-view clustering methods detect better circles than single-view clustering methods; second, by presuming the sparse social graphs are incomplete, our modified method detects better circles than the standard method that ignores such potential incompleteness. In particular, we believe a direct application of the standard method on a possibly incomplete graph may yield a biased result. By integrating theories from spectral clustering and matrix perturbation, we prove an information-theoretic upper bound for such bias and discuss how it may be affected by the characteristics of the social network.

1 Introduction

Online social networks are becoming extremely popular, attracting huge amounts of users and Internet traffic. For instance, Facebook recorded one billion active user accounts in late 2012, while approximately 10 million messages are posted every hour. They have significantly changed our information sharing and socialization behavior, especially among the younger generation – it has been reported that 48% percent of Facebook users between 18-34 years old check Facebook when they wake up¹. Effectively analyzing online social networks has

¹<http://www.statisticbrain.com/facebook-statistics/>

become critical for better understanding and promoting online socialization.

A fundamental and important problem in social network analysis is detecting social circles in *ego-nets* [33]. In a social network, an ego-net (or, abbreviated as *ego-net*) is a sub-network formed by all friends of a particular user. This user is called the *ego* and each friend is called an *alter*. A *social circle* is then a subset of the friends, which are usually similar in some sense. As suggested in [33], this notion has many potential applications such as content filtering or group recommendation. In particular, we notice in the user-center privacy and HCI research community, this concept was used to control the *information boundary* ([44]) of ego-nets in [46] so that an ego’s new messages are posted only to his friends in designated social circles. This control helps to alleviate the leak of the ego’s privacy such as location, which could be effectively inferred from his posts about local restaurants [29], containing location-indicating words like “Time Square” [11, 8], etc.

Although social circle has been commercialized in various products such as the circles in Google+ and custom lists in Facebook, most of them are not well-received by users. As pointed out in [33], a main reason is most of them require manual labeling of the social circles, which is usually tedious and labor-intensive. Therefore, it remains an important task to design effective methods for automatically detecting social circles in ego-nets.

Tracing this line of research, we notice two fundamental questions in the literature: how to detect overlapping circles and how to leverage node attributes (i.e. user profiles) for detection (e.g. [34, 7, 55]). There is also an attempt to use existing circles from other ego-nets for detecting the circles in a target ego-net [14]. These works, however, all consider a single view of the ego-net structure. In reality, the ego-net structure may be described from multiple views. For instance, one view may reveal the friend relationship between users, while another view may reveal how frequent they interact with each other (e.g. reply each other’s posts). This motivates us to ask a research question that is orthogonal to the existing ones, i.e. *how to effectively leverage the (usually available) multiple views of an ego-net structure for better social circle detection?*

To address the new question, we crawl ego-nets from Twitter and construct a graph for each with six views. These include two structural views regarding the friendship and common friends between alters, three interaction views regarding their replies, co-replies and re-tweets, and one content regarding the content similarity between their posts. We call each constructed graph a *multi-view social graph* in the following discussions. Note our views do not include the alter profiles (e.g. education, age and hobbies) used in most previous studies, as these information may not be available due to the alters’ privacy concern. Then, we introduce a multi-view spectral clustering method [27] to automatically detect circles from the multi-view social graph. By comparing its performance with those obtained from a single view or a naive concatenation of views, we show the introduced method finds better circles under several automatic and manual measurements.

During investigation, we had two observations: 1) many views of the social graphs are very sparse; 2) our modified multi-view spectral clustering method that selectively transfers information across views improves the performance on these graphs over the standard method. We conjecture these phenomena co-occur for the following reason: many present graphs/views are in fact incomplete due to the limited time of data collection or scarce use of alters, which

induces their sparseness; as a result, standard clustering method that ignores such potential incompleteness may give a result that deviates significantly from the optimal one. For better understanding the issue, we derive an information-theoretic bound for such deviation and discuss its implications on how the deviation may be affected by several characteristics of the ego-nets. Note we are not accusing the graph sparsity for causing the performance degeneration, but the potential incompleteness of these graphs that induce their sparseness.

The contributions of this paper are summarized as follows: we propose to automatically detect social circles in ego-nets based on the multiple views of their network structures; crawl and construct six views for the Twitter ego-nets; introduce a multi-view spectral clustering method to detect circles and show it performs better than single-view method with naive combination of views; modify the clustering method based on the sparse nature of the network and show it performs better than the original method; prove an information-theoretic bound for the deviation of results obtained by standard clustering method applied on a possibly incomplete ego-network.

The rest of the paper is organized as follows: the problem setting and main notations are introduced in section 2; the multi-view graph model of ego-nets is introduced in section 3; the multi-view spectral clustering methods and the deviation bound are presented in section 4; experimental studies are presented in section 5, followed by related works in section 6 and conclusion in section 7.

2 Notations and Problem Settings

For any matrix M , let M_{ij} be its entry at row i and column j , let $M_{:j}$ be its j_{th} column and $M_{i:}$ be its i_{th} row. Let M^T be its transpose, $\|M\|$ be its operator norm and $\|M\|_F$ be its Frobenius norm. When M is associated with a particular view t , we add a superscript $M^{(t)}$. For instance, $M_{ij}^{(t)}$ is an entry of the matrix associated with view t . Let I be an identify matrix properly sized by the context. For two matrices M, M' of the same size, let \succeq and \succ be the Loewner partial orders such that $M \succeq M'$ if $M - M'$ is positive semi-definite and $M \succ M'$ if $M - M'$ is positive definite, and $M \circ M'$ be their Hadamard product. For an integer ℓ , define notation $[\ell] := \{1, 2, \dots, \ell\}$.

Recall an ego network is the network formed by all friends of a particular user. The user is called the *ego* and each friend is called an *alter*. The network is represented by a graph, where each node represents an alter and each edge represents a connection between two alters. Different types of connections form different views of the graph.

The view t of a graph is characterized by a similarity matrix $K^{(t)} \in \mathbb{R}^{n \times n}$, where n is the number of alters and $K_{ij}^{(t)}$ is the ‘similarity’ between alters i and j under this view. (The similarities will be defined in the next section.) When an arbitrary view is being referred, the superscript t will be omitted. For instance, K_{ij} represents the similarity between two alters in an arbitrary view. Such omission is mainly used in theoretical analysis.

Given an ego-net characterized by a multi-view graph $\{K^{(t)}\}_{t \in [T]}$ of T views, our task is to automatically detect social circles based *solely* on this graph. (No alter profile is needed.) For simplicity, we focus on non-overlapping circles and the extension to overlapping circles is discussed later.

3 Multiple Views of the Ego-Net Structure

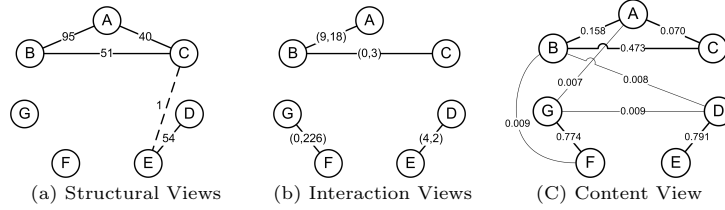


Figure 1: A Real World Online Social Sub-Network. In (a), a solid line between two users indicate they are friends (follow each other), and its label is the number of common friends between them; a dash line with a label means two users are not friends but have common friends. In (b), a solid line labeled by (a, b) means its connected users have a replies and b re-tweets to each other in total. In (c), a solid line labeled by a means the connected users have content similarity a . We only display edges with label greater than 0.0065, and the thicker edge has similarity greater than ≥ 0.01 . The computations of all labels are specified in Section 3.2.

3.1 A Motivating Example

An advantage of considering multiple views of the ego-net structure is that different views provide complementary information for more effective discovery of hidden social circles. Figure 1 shows an example crawled from Twitter.

The figure shows a sub-network in an ego-net, which contains six alters marked as letters A, B, C, D, E, F and and five views of the ego-net structure. These include three types of views: 1) two structural views indicating whether two alters are friends and how many friends they have in common respectively; 2) two interaction views indicating how many times two alters reply to and retweet each other respectively; 3) a content view indicating how similar are the posts of two alters.

On one hand, we see different types of views are partly consistent in indicating the similarity between alters. For example, alters A and B are strongly connected in the structural views, which coincides with their frequent interactions; alters C and D have no connection in the structural view, nor any interaction or similarity in content.

3.2 View Construction and Cluster Assumption

In total we construct six views for the ego-nets crawled from Twitter. These include two structural views, three interaction views and one content view.

Friendship. This view characterizes the friend relationship between alters. Its similarity matrix $K^{(1)}$ is defined as $K_{ij}^{(1)} = 1$ if alters i and j follow each other on Twitter, and $K_{ij}^{(1)} = 0$ otherwise.

Common Friend. This view characterizes how many friends are shared between alters. Its similarity matrix $K^{(2)}$ is defined as $K_{ij}^{(2)} = m$ if alters i and j have m friends in common. Note alters i and j themselves are not counted.

Reply. This view characterizes how many times alters reply to each other. Its similarity matrix $K^{(3)}$ is defined as $K_{ij}^{(3)} = r_{i \rightarrow j} + r_{j \rightarrow i}$ where $r_{p \rightarrow q}$ presents the number of times alter p replies to alter q .

It is noted the similarity matrix $K^{(3)}$ is symmetric due to the requirement of standard spectral clustering methods (e.g. [49, section 2.1]). However, this does not necessarily imply we have represented the user replies as an undirected graph. Instead, its symmetry is open to interpretations: one could indeed view it as the adjacent matrix (also the similarity matrix) of an undirected graph of user replies, or as the similarity matrix obtained from the adjacent matrix of a directed graph. In the second interpretation, the underlying adjacent matrix could be $\tilde{K}^{(3)}$, where $\tilde{K}_{ij}^{(3)}$ is the number of replies from alter i to alter j . Then, we choose to achieve symmetry by $K^{(3)} = \tilde{K}^{(3)} + (\tilde{K}^{(3)})^T$ for simplicity, and there are many other options to do so. In all cases, $K^{(3)}$ would be symmetric for standard spectral clustering. The same argument applies to the following similarity matrices of co-reply and re-tweet.

Co-Reply. This view characterizes how many times alters co-reply the posts. Its similarity matrix $K^{(4)}$ is defined as $K_{ij}^{(4)} = m$ if alters i and j co-reply m posts on Twitter.

Re-tweet. This view characterizes how many times alters retweet each other's posts. Its similarity matrix $K^{(5)}$ is defined as $K_{ij}^{(5)} = r'_{i \rightarrow j} + r'_{j \rightarrow i}$ where $r'_{p \rightarrow q}$ presents the number of times alter p retweets alter q 's posts.

Topic. This view characterizes the similarity of topics posted by alters. Its similarity matrix $K^{(6)}$ has entry $K_{ij}^{(6)}$ defined as the cosine distance between the 'topic vectors' of alters i and j . The topic vector of each alter is obtained as follows: first, we crawled his posts on Twitter and uploaded to the online annotation tool TagMe [15], which returns a set of related topics on Wikipedia as well as their scores of relevance; then, we represent each alter by a vector, where each dimension corresponds to the relevance score of one topic (that is relevant to the posts of at least one alter); finally, from these vectors we obtain their TF-IDF weight vectors, which are used as the topic vectors of the alters.

It is tempted to ask if TF-IDF is proper for our application, considering it may lower the weights of topics that are popular within the ego-net. Indeed, if the ego has a high interest in sports and only connect to people talking about sports, then topic 'sport' may have low TF-IDF weight while any peripheral topic such as 'cooking' may gain higher weight and thus has higher impact on the clustering result.

We view the above situation from four aspects. First, if the ego connects only to people talking about a popular topic, then there is no need to form a circle about that topic. (The ego does not need to be reminded that all his alters love sports.) Instead, we believe those less popular yet more diverse topics are the very reason for differentiating and grouping alters into circles. Second, if all alters share a common topic such as sports, there would be a big pool of related sub-topics such as basketball, football and swimming. These topics would gain higher TF-IDF weights and effectively differentiate the alters. Comparatively, the very peripheral topics may have lower TF-IDF due to their very scarce presence. Finally, automatic social circle detection is not merely a way of speeding up manual circle detection. It could also be 'intelligent', in the sense of discovering and recommending circles that the ego may not even be aware of so as to enrich his information and improves his decisions. Therefore,

if there really exists a considerable number of alters talking about cooking (so this topic gains sufficiently large TF-IDF), it shall make sense to alter the ego about the existence of such potential circle. Finally, it should be mentioned our clusters are detected based on six views of the ego-net structure, but not only the topic view. If the ‘cooking’ alters are not similar in other views, then a ‘cooking’ circle is less likely to be form. However, if these alters turn out to have high similarities in other views, it makes sense to form a circle for them.

Cluster Assumption. We expect alters in the same social circles to have higher similarity in multiple views (as compared with those in different circles). This means they are more likely to be friends, share more common friends, retweet or reply to each other more often, co-reply to the same messages more usually, and post messages with more similar topics. This is similar to the assumption made in [34].

4 Clustering on Multi-View Ego-Net

In this section, we employ and design multi-view spectral clustering techniques to automatically detect social circles. This family of techniques has proved to be effective in performing clustering on graphs (e.g. [25, 26]).

We first briefly review a popular and standard method [25], which treats the our observed ego-net as a complete one. During investigation, however, we found modifying this method by assuming the (very sparse) ego-net is incomplete improved the clustering performance. This inspired us to conjecture the observed ego-net is inherently incomplete and a direct application of standard method may yield a result that deviates from the optimal one. To better under the issue, we derive an upper bound for such deviation and discuss its implications on how the ego-net characteristics may affect the deviation. Finally, we present a modification of the standard method that assumes the ego-net is incomplete and selectively transfers information across views.

4.1 Co-Trained Spectral Clustering: A Revisit

Spectral clustering is a popular technique to cluster a set of points based *solely* on their similarities. These similarities are represented as a graph, where each node is a point (alter) and each edge is the similarity between its connecting points. It has been shown the corresponding graph Laplacian matrix has principal eigen-vectors containing discriminative information for partitioning the nodes (e.g. [39]). Therefore, spectral clustering uses these eigenvectors as latent features and performs standard clustering techniques such as K-means based on them.

Multi-view spectral clustering aims to leverage the multiple views of a graph to improve the clustering quality. The main idea is to find clusters that are largely consistent across various views. (Recall the example in Figure 1.) In this paper, we employ a popular method called *co-trained spectral clustering (csc)* [25]. It imposes consistency by alternately using the principal eigen-vectors of one view to refine the similarity matrices of other views. Let $U_{:, [k]}^{(t)}$ be the matrix whose columns are the leading k eigen-vectors of the normalized Laplacian matrix of $K^{(t)}$. (Detailed definition will be given later.) Then, the similarity

matrix of another view t' is refined by

$$K^{(t')} = U_{:[k]}^{(t)} \left(U_{:[k]}^{(t)} \right)^T K^{(t')}. \quad (1)$$

Intuitively, the above update re-represents $K^{(t')}$ in the space spanned by $U_{:[k]}^{(t)}$, and the authors showed this may achieve view consistency by throwing away the within-cluster details of each view that may confuse clustering. When the alternate update converges, the eigen-vectors of all (or, dominant) views are concatenated to form a latent feature, based on which standard K-means is performed to partition the nodes.

It is noted that due to the possible noise and limited observations in view t , it is possible $U_{:[k]}^{(t)}$ may not be accurately estimated and its application on other views in (1) may mis-refine their similarity matrices. The same problem exists for our later modification of this method. This is an inherent limitation of the family of multi-view learning methods. For instance, it is possible that a co-training classifier [6] may mislabel an unlabeled data when the training sample is scarce, but this pseudo-label would be used permanently to refine both the current view and the other view. It is perhaps for this very reason that strong assumptions such as classifier is ‘never confident but wrong’ in classification has to be made for theoretical analysis [3]. However, this problem is beyond the scope of our investigation and no further discussion would be presented.

4.2 Standard Clustering on An Incomplete Graph

Through empirical studies, we conjecture the observed ego network is inherently incomplete. Therefore, directly applying standard *csc* that ignores such incompleteness may yield a result that deviates significantly from the optimal one. For better understanding the issue, we derive an upper bound for such deviation and discuss its implications on how the deviation may be affected by the network characteristics. Since *csc* can be essentially viewed as single-view spectral clustering on a dominant view (which is refined by other views), our analysis will focus on the single-view case and its implications for the multi-view case will be briefly discussed later.

4.2.1 A Deviation Bound and its Implications

First, we make a *free-approximation* assumption to simplify discussion. It is well known spectral clustering is an approximated solution to the optimal normalized cut problem, and there is a rich literature studying the approximation error (e.g. [43, 58]). Although we apply spectral clustering and evaluate the result under the optimal cut framework, such approximation is not our focus. We thus assume the approximation error is zero, which could be satisfied if the leading k eigen-vectors of the graph Laplacians are piece-wise constant with respect to the optimal normalized cut result [23]. When the assumption is not satisfied, our analysis could be generalized by simply adding an additional approximation term.

Next, we introduce a few more notations. Consider k -partitioning over n nodes on a complete graph with similarity matrix K . Let

$$L = D^{-1/2} K D^{-1/2} \quad (2)$$

be the Laplacian matrix ², where $D \in \mathbb{R}^{n \times n}$ is a diagonal matrix such that $D_{ii} = \sum_{j \in [n]} K_{ij}$. Let σ_k and λ_k be the k_{th} leading eigenvalues of D and L respectively.

Let \tilde{K} be an incomplete observation of K indexed by some set Ω such that, $\tilde{K}_{ij} = K_{ij}$ if $(i, j) \in \Omega$ and $\tilde{K}_{ij} = 0$ otherwise. Note $\tilde{K}_{ij} = 0$ may imply either K_{ij} is not observed or K_{ij} is observed yet takes value 0. Similarly, let $\tilde{L} = \tilde{D}^{-1/2} \tilde{K} \tilde{D}^{-1/2}$ be the Laplacian of \tilde{K} , where \tilde{D} is a diagonal matrix with $\tilde{D}_{ii} = \sum_{j \in [n]} \tilde{K}_{ij}$.

To represent the partition results, let $\mathcal{V} \in \mathbb{R}^{n \times k}$ be the indicator matrix for a k -partition on graph K such that $\mathcal{V}_{ij} = 1$ if node i is assigned to the j_{th} cluster and $\mathcal{V}_{ij} = 0$ otherwise. Similarly, let $\tilde{\mathcal{V}}$ be the indicator matrix for a k -partition on graph \tilde{K} . Similar to [2, Formula (2)], we evaluate the difference between these two partitions using the metric

$$d(\mathcal{V}, \tilde{\mathcal{V}}) = \frac{1}{2} \left\| \sum_{j \in [k]} \frac{\mathcal{V}_{:j} (\mathcal{V}_{:j})^T}{(\mathcal{V}_{:j})^T \mathcal{V}_{:j}} - \sum_{j' \in [k]} \frac{\tilde{\mathcal{V}}_{:j'} (\tilde{\mathcal{V}}_{:j'})^T}{(\tilde{\mathcal{V}}_{:j'})^T \tilde{\mathcal{V}}_{:j'}} \right\|_F^2. \quad (3)$$

Intuitively, this metric counts the number of node pairs assigned to different clusters, weighted by the sizes of the corresponding clusters. Indeed, note if nodes i_1 and i_2 are assigned to cluster j , then $(\mathcal{V}_{:j} (\mathcal{V}_{:j})^T)_{i_1 i_2} = 1$; and the size of cluster j is $(\mathcal{V}_{:j})^T \mathcal{V}_{:j}$.

Our deviation bound is stated as follows.

Proposition 1 *Suppose $\mathcal{V}, \tilde{\mathcal{V}}$ are the indicator matrices for the optimal normalized cut based on K, \tilde{K} respectively. Let $\tilde{\sigma}_1$ be the largest eigenvalue of $D - (D\tilde{D})^{1/2}$ and define $\tilde{\Delta} = L - \tilde{L}$. Then*

$$d(\mathcal{V}, \tilde{\mathcal{V}}) \leq \frac{\sigma_1}{\sigma_n} \left(\frac{\tilde{\sigma}_1}{\sigma_n} + \frac{2 \min\{\sqrt{k} \|\tilde{\Delta}\|_2, \|\tilde{\Delta}\|_F\}}{\lambda_k - \lambda_{k+1}} \right). \quad (4)$$

The bound has several implications. First, we notice $\sigma_1, \sigma_n, \lambda_k, \lambda_{k+1}$ are all constants when an underlying complete graph is given. Their impacts on the bound can be interpreted as follows. Since σ_1 is the largest sum of entries in one row of K , we could interpret it as the total behavior of the most active alter in the ego-net ³ Likewise, σ_n indicates the total behavior of the laziest alter. Then, the ratio σ_1/σ_n in (4) suggests a standard clustering method may suffer less deviation when applying on an incomplete graph, if the alters are behaving (in total) equally active in the ego-net. On the other side, the bound decreases as the eigen-gap $\lambda_k - \lambda_{k+1}$ increases. Since concentrated graphs usually have sharper eigen-gaps, we may expect less deviation when alters have non-uniform behaviors with each other (while their total behaviors remain equally active).

Second, our bound suggests the choice of k for lowering the risk of deviation. By \sqrt{k} in (4), we see detecting fewer social circles may suffer less deviation. By $\lambda_k - \lambda_{k+1}$, on the other hand, we see one may choose k at the ‘steepest’ location

²A more classic definition is $L = I - D^{-1/2} K D^{-1/2}$. Our definition is taken from [39], which admits the same set of eigenvectors used in analysis yet greatly facilitates discussions.

³Our discussion applies to an arbitrary view. In interaction views, an ‘active’ alter interacts frequently with other alters; in other views, such alter may have many friends or similar interests with many other alters.

of the graph spectrum. To be more specific, when the alters behaves (after normalization) equally active, the graph spectrum degrades slower and we may choose a relatively large k ; otherwise a smaller k is more desirable.

The bound also sheds light on how the incomplete observation may affect the deviation. As more alter behaviors are observed, it is clear that $\tilde{K} \rightarrow K$ ⁴. This implies $\tilde{D} \rightarrow D$ and $\tilde{L} \rightarrow L$, which further implies $\tilde{\sigma}_1 \rightarrow 0$ and $\Delta \rightarrow 0$ respectively, yielding smaller deviation bounds. In particular, once the observation is complete, $\tilde{\sigma}_1 = 0$ and $\Delta = 0$, in which case no deviation would be suffered. Moreover, since $\tilde{\sigma}_1$ is the largest diagonal entry of $D - (D\tilde{D})^{1/2}$, it is likely to be caused by the ‘laziest-active’ alter in the ego-net, i.e. the user who has great interest in interacting with others but cannot afford to use social networks too often due to his/her busy schedule. It shall make sense to see larger $\tilde{\sigma}_1$ may be implied when such user does exist in the ego-net.

Finally, the bound provides some theoretical support for applying multi-view spectral clustering methods. As suggested by the example in Figure 1, various views may complement each other, partly filling the missing observations. We note, however, the direction of information transfer across views is critical. Consider information transfer from view t' to a dominant view t . If $\tilde{K}_{ij}^{(t)} = 0$ but $\tilde{K}_{ij}^{(t')} > 0$, then increasing $\tilde{K}_{ij}^{(t)}$ to reach view consistency helps to achieve $\tilde{K}^{(t)} \rightarrow K^{(t)}$ and thus reduce the performance deviation. However, if $\tilde{K}_{ij}^{(t)} > 0$ but $\tilde{K}_{ij}^{(t')} = 0$, decreasing $\tilde{K}_{ij}^{(t)}$ may increase the deviation because it is possible $\tilde{K}_{ij}^{(t')}$ is unobserved. (For simplicity, we assume the underlying complete multi-view graph has view consistency.) The standard clustering method *csc* ignores such difference and equally transfer information in both directions, which may increase the performance deviation. Our discussion here, however, suggests a conservative yet safer transfer scheme: when $\tilde{K}_{ij}^{(t')} > 0$, we transfer it to other views for enforcing view consistency; when $\tilde{K}_{ij}^{(t')} = 0$, we do not transfer it to other views. In section 4.3, we present a modified *csc* method that realizes such transfer scheme.

4.2.2 Proof of Proposition 1

Notations. Recall for an n -by- n similarity matrix K , we denote by L its Laplacian and by D the corresponding diagonal matrix; λ_k and σ_k are the k_{th} largest eigenvalues of L and D , respectively; \mathcal{V} is the indicator matrix of a k -partition based on K . Next, let $L = U\Lambda U^T$ be the eigen-decomposition of L , where $\Lambda \in \mathbb{R}^{n \times n}$ is the diagonal matrix with λ_k on its diagonal (sorted in descending order) and $U \in \mathbb{R}^{n \times n}$ is a unitary matrix whose columns are the corresponding eigenvectors. Let $U_{[k]} \in \mathbb{R}^{n \times k}$ be a submatrix of U which contains the top k principal eigenvectors. Note $U_{[k]}$ is orthonormal. Then, $\mathbb{P}_k = U_{[k]}U_{[k]}^T$ is the orthogonal projection onto the range space of $U_{[k]}$ (e.g. [19, Chapter 2]).

All above notations apply to another similarity matrix \tilde{K} , yet capped with a ‘ \sim ’ notation. For instance, $\tilde{\mathbb{P}}_k$ is the orthogonal projection onto the range space of $\tilde{U}_{[k]}$, which contains the top k principal eigenvectors of the Laplacian \tilde{L} .

Finally, let \succeq, \succ be the Loewner partial orders such that $A \succeq B$ if $A - B$ is positive semi-definite (PSD) and $A \succ B$ if $A - B$ is positive definite. Note $A \succeq 0$ implies A is PSD.

⁴Notation $A \rightarrow B$ means A_{ij} approaches B_{ij} for all indices (i, j) .

Proof Sketch. We first use triangular inequality to bound $d(\mathcal{V}, \tilde{\mathcal{V}})$ by two new terms; then bound the first term using perturbation theory [57] and the second term using properties of the Loewner partial orders (e.g. [20, Chapter 7]). Some results are also borrowed from [23].

Step 1: bound $d(\mathcal{V}, \tilde{\mathcal{V}})$. By [2, Formula (3)] we have

$$d(\mathcal{V}, \tilde{\mathcal{V}}) \leq \frac{\sigma_1}{\sigma_n} \cdot d(D^{1/2}\mathcal{V}, D^{1/2}\tilde{\mathcal{V}}). \quad (5)$$

Further, by triangular inequality it follows

$$d(D^{1/2}\mathcal{V}, D^{1/2}\tilde{\mathcal{V}}) \leq d_w(\mathcal{V}, \tilde{\mathcal{V}}) + d(\tilde{D}^{1/2}\tilde{\mathcal{V}}, D^{1/2}\tilde{\mathcal{V}}), \quad (6)$$

where $d_w(\mathcal{V}, \tilde{\mathcal{V}}) := d(D^{1/2}\mathcal{V}, \tilde{D}^{1/2}\tilde{\mathcal{V}})$.

Step 2: bound $d_w(\mathcal{V}, \tilde{\mathcal{V}})$. It is known that spectral clustering is a relaxation of the optimal normalized cut problem. In [2, Formula (1)], the relaxation error is measured by the difference between the orthogonal projection operators induced from the two problems. In our setting, these two operators (w.r.t. similarity matrix K) are \mathbb{P}_k and

$$\Pi_k := \sum_{j \in [k]} D^{1/2} \mathcal{V}_j \mathcal{V}_j^T D^{1/2} / (\mathcal{V}_j^T D \mathcal{V}_j). \quad (7)$$

By the free-approximation assumption, we have $\mathbb{P}_k = \Pi_k$. In a similar manner, the two operators for \tilde{K} are $\tilde{\mathbb{P}}_k$ and $\tilde{\Pi}_k := \sum_{j \in [k]} \tilde{D}^{1/2} \tilde{\mathcal{V}}_j \tilde{\mathcal{V}}_j^T \tilde{D}^{1/2} / (\tilde{\mathcal{V}}_j^T \tilde{D} \tilde{\mathcal{V}}_j)$. Since by definition

$$d_w(\mathcal{V}, \tilde{\mathcal{V}}) = \|\Pi_k - \tilde{\Pi}_k\|_F^2, \quad (8)$$

it follows

$$d_w(\mathcal{V}, \tilde{\mathcal{V}}) = \|\mathbb{P}_k - \tilde{\mathbb{P}}_k\|_F^2. \quad (9)$$

Now, our problem becomes bounding $\|\mathbb{P}_k - \tilde{\mathbb{P}}_k\|_F^2$ instead. A classic approach is to apply the *Davis-Kahan sin θ* theorem (e.g. [57, Theorem 1]) so that

$$\|\mathbb{P}_k - \tilde{\mathbb{P}}_k\|_F \leq \frac{\|\Delta\|_F}{\kappa}, \quad (10)$$

where $\kappa = \inf\{|\lambda_i - \tilde{\lambda}_j|; 1 \leq i \leq k, k < j \leq n\}$.⁵ While this bound is seminal, it contains an implicit dependency on Δ through parameter $\tilde{\lambda}$, whereas we favor a bound that has more explicit dependency on Δ for easier interpretation. To this end, we apply a recent generalization of the classic *sin θ* theorem, stated as follows.

Theorem 1 ([57, Theorem 2]) *Let $L, \tilde{L} \in \mathbb{R}^{n \times n}$ be symmetric, with eigenvalues $\lambda_1 \geq \dots \geq \lambda_n$ and $\tilde{\lambda}_1 \geq \dots \geq \tilde{\lambda}_n$ respectively. Fix $1 \leq r \leq s \leq n$ and assume that $\min\{\lambda_{r-1} - \lambda_r, \lambda_s - \lambda_{s+1}\} > 0$, where $\lambda_0 := \infty$ and $\lambda_{n+1} := -\infty$. Let $d := s - r + 1$ and let $U_k = [u_r, u_{r+1}, \dots, u_s] \in \mathbb{R}^{n \times d}$ and $\tilde{U}_d = [\tilde{u}_r, \tilde{u}_{r+1}, \dots, \tilde{u}_s] \in \mathbb{R}^{n \times k}$ have orthonormal columns satisfying $Lu_j = \lambda_j u_j$ and $\tilde{L}\tilde{u}_j = \lambda_j \tilde{u}_j$ for $j = r, r+1, \dots, s$. Then*

$$\|\mathbb{P}_k - \tilde{\mathbb{P}}_k\|_F \leq \frac{2 \min(\sqrt{d}\|\Delta\|_2, \|\Delta\|_F)}{\min\{\lambda_{r-1} - \lambda_r, \lambda_s - \lambda_{s+1}\}}. \quad (11)$$

⁵The original theorem bounds the angles between subspaces, which equals the difference of their orthogonal projectors, e.g. [13, Page 10].

By (9) and Theorem 1 (with $r = 1$ and $s = k$), we have

$$d_w(\mathcal{V}, \tilde{\mathcal{V}}) \leq \frac{4 \min(\sqrt{k} \|\Delta\|_2^2, \|\Delta\|_F^2)}{(\lambda_k - \lambda_{k+1})^2}. \quad (12)$$

Step 3: bound $d_+ := d(\tilde{D}^{1/2} \tilde{\mathcal{V}}, D^{1/2} \tilde{\mathcal{V}})$. First, it is easy to verify the following lemma by simple algebra.

Lemma 1 *For any orthogonal matrix $M \in \mathbb{R}^{n \times p}$,*

$$\sum_{j \in [p]} M_{:,j} M_{:,j}^T / (M_{:,j}^T M_{:,j}) = M(M^T M)^{-1} M^T. \quad (13)$$

Note $D^{1/2} \tilde{\mathcal{V}}$ and $\tilde{D}^{1/2} \tilde{\mathcal{V}}$ are orthogonal. Then, jointly applying Lemma 1 and the alternative expression in [2, Page 6] for $\|M(M^T M)^{-1} M^T - \tilde{M}(\tilde{M}^T \tilde{M})^{-1} \tilde{M}^T\|_F^2$, we have

$$d_+ = \text{tr}\{\mathcal{T}^{-1/2}(\mathcal{T} - \tilde{\mathcal{N}})\mathcal{T}^{-1/2}\}, \quad (14)$$

where $\mathcal{T} = \tilde{\mathcal{V}}^T D \tilde{\mathcal{V}}$ and

$$\tilde{\mathcal{N}} = \tilde{\mathcal{V}}^T (D \tilde{D})^{1/2} \tilde{\mathcal{V}} (\tilde{\mathcal{V}}^T \tilde{D} \tilde{\mathcal{V}})^{-1} \tilde{\mathcal{V}}^T (\tilde{D} D)^{1/2} \tilde{\mathcal{V}}. \quad (15)$$

It the sequel, we bound $\mathcal{T}^{-1/2}$ and $\mathcal{T} - \tilde{\mathcal{N}}$ separately.

Note $\tilde{\mathcal{V}}$ and $D^{1/2} \tilde{\mathcal{V}}$ have linearly independent columns (since $\tilde{\mathcal{V}}$ indicates a partition of nodes and $D^{1/2}$ does not change such indication). Then, by [20, Theorem 7.2.10]

$$\mathcal{T} = \tilde{\mathcal{V}}^T D \tilde{\mathcal{V}} \succ 0 \quad \text{and} \quad \tilde{\mathcal{V}}^T \tilde{\mathcal{V}} \succ 0. \quad (16)$$

Further, since σ_n is the smallest diagonal entry of D , it is easy to verify $D \succeq \sigma_n I$. This implies

$$\mathcal{T} \succeq \sigma_n \tilde{\mathcal{V}}^T \tilde{\mathcal{V}}. \quad (17)$$

Based on (16) and (17), by [20, Corollary 7.7.4] we have

$$\sigma_n^{-1/2} (\tilde{\mathcal{V}}^T \tilde{\mathcal{V}})^{-1/2} \succeq \mathcal{T}^{-1/2}. \quad (18)$$

It remains to bound $\mathcal{T} - \tilde{\mathcal{N}}$. By definition

$$(D \tilde{D})^{1/2} \succeq \tilde{D}, \quad (19)$$

which implies $(\tilde{\mathcal{V}}^T \tilde{D} \tilde{\mathcal{V}})^{-1} \succeq (\tilde{\mathcal{V}}^T (D \tilde{D})^{1/2} \tilde{\mathcal{V}})^{-1}$. Plugging this in (15), we have

$$\tilde{\mathcal{N}} \succeq \tilde{\mathcal{V}}^T (D \tilde{D})^{1/2} \tilde{\mathcal{V}}. \quad (20)$$

Therefore,

$$\tilde{\sigma}_1 \tilde{\mathcal{V}}^T \tilde{\mathcal{V}} \succeq \tilde{\mathcal{V}}^T (D - (D \tilde{D})^{1/2}) \tilde{\mathcal{V}} \succeq \mathcal{T} - \tilde{\mathcal{N}}, \quad (21)$$

where $\tilde{\sigma}_1$ is the largest diagonal entry of $D - (D \tilde{D})^{1/2}$. Combining (18) and (21) gives

$$\sigma_n^{-1} \tilde{\sigma}_1 I \succeq \mathcal{T}^{-1/2} (\mathcal{T} - \tilde{\mathcal{N}}) \mathcal{T}^{-1/2}. \quad (22)$$

Taking trace on both sides yields

$$\sigma_n^{-1} \tilde{\sigma}_1 \geq d_+. \quad (23)$$

Step 4: combining (5, 6, 12, 23) proves the proposition.

Algorithm 1 Selective Co-trained Spectral Clustering

Input: Similarity matrices of T views K_1, K_2, \dots, K_T
Initialize: For all $t \in [T]$, $U^{(t)} = \text{eig}(K^{(t)}, k)$ and $C^{(t)} = \text{clust}(U^{(t)}, k)$
for $i = 1$ **to** rounds **do**
 for $t \in [T]$ **do**
 2: Refine similarity matrix $K^{(t)} = \text{update}(t) \circ K^{(t)}$
 3: Update $U^{(t)} = \text{eig}(K^{(t)}, k)$
 4: Update $C^{(t)} = \text{clust}(U^{(t)}, k)$
 end for
end for
Output: apply K-means on the concatenated feature matrix $U := [U^{(k_1)}, U^{(k_2)}, \dots, U^{(k_\ell)}]$, where k_1, k_2, \dots, k_ℓ are the views of major interest.

4.3 Selective Co-trained Spectral Clustering

As suggested by prior discussions, one way to avoid the increase of deviation bound is to transfer clustering results of *only* observed entries across views. In practice, however, this prior knowledge may be difficult to obtain.

In this section, we present a heuristic that modifies the standard *csc* to realize selective transfer from two aspects: first, one view is considered incomplete (in general) if its similarity matrix is very sparse; second, in an incomplete view an entry is considered observed if it has non-zero value. We expect such heuristic to lower the risk of transferring unobserved entries across views, at the cost of sacrificing some view consistency. To be more specific, the only case we may miss is when two alters have no similarity in one view but high similarities in other views. In this case, our modified method will not lower the similarities in other views (as standard method will). Based on the view consistency assumption, however, this may not happen too often and thus the loss of performance improvement may not be significant.

For conciseness, define three functions and notations.

(1) $\text{eig}(K, k) := U \in \mathbb{R}^{n \times k}$. This function performs eigen-decomposition on the normalized Laplacian of K defined in (2). Columns of U are the top k eigen-vectors of the Laplacian.

(2) $\text{clust}(U, k) := C \in \mathbb{R}^{n \times n}$. This function takes U as the latent feature matrix of n points and performs K-means clustering. Each row of U is treated as the feature vector of one point; $C_{ij}=1$ if points i and j are assigned to the same cluster and $C_{ij}=-1$ otherwise.

(3) $\text{update}(t) := \exp \sum_{\substack{t' \in [T] \\ t' \neq t}} C^{(t')} \circ (\mathbf{1}\{K^{(t')} \neq \mathbf{0}\})^{\delta_{t'}}$. This function returns an

n -by- n matrix for updating the similarity matrix of view t . Here, $C^{(t')}$ is the matrix returned by $\text{clust}(U^{(t')}, k)$; $\mathbf{1}\{\cdot\}$ is an element-wise indicator function; $\delta_{t'}$ is a binary constant taking value 1 if $K^{(t')}$ is sufficiently sparse and taking value 0 otherwise. In practice we set a threshold to determine whether a matrix is sufficiently sparse (i.e. whether it has sufficient zero entries).

Our modified *csc* method is presented in Algorithm 1. Its major component is the updating matrix $\text{update}(t)$, which is designed based on the following three intuitions.

Term $C^{(t')}$: if alters i and j are assigned to the same cluster in view t' , we

have $C_{ij}^{(t')} = 1$. This makes $update(t)_{ij} > 1$, which will increase the similarity $K_{ij}^{(t)}$ in view t by the algorithm. Similarly, if alters i and j are assigned to different clusters in view t' , the algorithm decreases $K_{ij}^{(t)}$ for view consistency.

Term $\mathbf{1}\{K^{(t')} \neq \mathbf{0}\}$: if alters i, j have non-zero similarity $K_{ij}^{(t')} \neq 0$, then $(\mathbf{1}\{K^{(t')} \neq \mathbf{0}\})_{ij} = 1$ and so their clustering result $C_{ij}^{(t')}$ will be transferred to other views (conditioned on $\delta_{t'} = 1$); otherwise, their clustering result will not be transferred.

Term $\delta_{t'}$: if view t' is considered sparse, then $\delta_{t'}$. This will activate the ‘selective’ function $\mathbf{1}\{K^{(t')} \neq \mathbf{0}\}$ to selective use results in view t' to refine the other views; otherwise, the selective function is de-activated and all results in view t' are transferred.

Finally, we briefly discuss the convergence property of the proposed algorithm. Consider the problem of clustering three alters based on two views. Suppose the result based on view one is

$$C^{(1)} = \begin{bmatrix} 1 & -1 & 1 \\ -1 & 1 & -1 \\ 1 & -1 & 1 \end{bmatrix}, \quad (24)$$

which implies alter 1 and 3 are similar while alters 2 and 3 are not. Suppose further the similarity matrix of view two is

$$K^{(2)} = \begin{bmatrix} 1 & 0.4 & 0.1 \\ 0.4 & 1 & 0.6 \\ 0.1 & 0.6 & 1 \end{bmatrix}. \quad (25)$$

After refining the second view based on the clustering result in view one, we have an updated similarity matrix

$$K^{(2)} = \begin{bmatrix} 2.7 & 0.2 & 0.3 \\ 0.2 & 2.7 & 0.2 \\ 0.3 & 0.2 & 2.7 \end{bmatrix}. \quad (26)$$

It is clear the algorithm lowers the similarity between alters 2 and 3. However, the similarity between alters 1 and 3 are not significantly boosted due to their strong evidence of dissimilarity in view two. This suggests the proposed algorithm may effectively modify alters whose similarities are uncertain in some views, but it does not enforce view consistency on similarities that are strongly against each other in different views. One strongest disagreement occurs when one view has zero similarity whereas the other view has non-zero similarity. In this case, we expect our selective algorithm to converge faster, since it does not enforce view consistency between observed and (possibly) unobserved similarities that may mislead learning. In experiment, we show this is indeed the case. Note since $C^{(1)}$ is symmetric, the refined similarity matrix $K^{(2)}$ remains symmetric. (Thus its corresponding Laplacian matrix remains positive semi-definite and has positive eigenvalues.)

5 Experimental Study

5.1 Data Collection and View Construction

Twitter and Facebook are perhaps the most popular social networks considering their number of active users and daily traffic. Since Facebook users mostly use real identities, it enforces privacy protection constraints that prevent us from collecting a large amount of data. For this reason, we will evaluate our methods on Twitter and implemented a crawler to collect Twitter data using its API, which can return any user’s profile, follower/following lists and tweets. The user profile consists of user name, screen name, user id, profile create time, description (a personal statement), location and time zone. The tweets information consists of tweet id, post time, tweet location, in-reply-to user id, in-reply-to status id, list of re-tweets (user id and tweet id) and tweet content. For each user, we only collected his/her most recent 2000 tweets due to many constraints. It is also noted not all the attributes are available and accurate for all users. For example, user location in user profiles is self-generated textual description, where we have seen “Worldwide”, and “Coming Soon Everywhere” etc. Meanwhile, tweet locations are accurate latitudes and longitudes, but they are missing from most of the tweets. Finally, Twitter has enforced mandatory limits on the crawling rate, especially for crawling account-specific information. We have collected 92 data sets – 92 seed users and all their friends. In our data set, each seed user has 245 friends on average. In total, we have collected information of more than 22K users, with approximately 3 million friendship links, and more than 27 million tweet messages.

In section 2, we have defined six views of the ego-network structure. Here, we provide further details on how each view is constructed based on the collected data.

Friendship. For two alters, if each of them is in both the follower and following lists of the other, then they are considered as friend.

Common Friend. We define the friend list of an alter as the intersection of his follower list and following list. Then, the number of common friends between two alters is the cardinality of the intersection of their friend lists.

Reply. For two alters, we scan through one’s posts and count the number of replies from the other. The same scheme is applied to the opposite direction, and the sum of the two numbers is used as the reply number between the two alters.

Co-Reply. For two alters, we scan through all tweets in the crawled ego-net and count the number of posts that they both replied.

Re-tweet. For two alters, we scan through one’s posts and count how many were retweeted by the other. The same scheme is applied to the opposite direction, and the sum of the two numbers is used as the re-tweet number between two alters.

Content. For an alter, we first collect his posts (and profiles if available) in the ego-net to form a corpus. Then, TagMe [15] is used to find its relevant topics and the TF-IDF based topic vector is constructed for the alter (as explained in section 2.3). In experiment, each topic returned by TagMe is scored between $[0, 1]$, indicating its relevance to the corpus. Following the Pareto principle, we remove topics with scores lower than 0.2 (approximately removing 80% of the low-confidence tags).

Finally, after each similarity matrix K is constructed, we normalize it into $[0, 1]$ by dividing all entries by the maximum entry and fixing the diagonal entries to 1 (indicating that self-similarity is always the highest among all).⁶

5.2 Protocol

We implement the proposed selective co-trained spectral clustering (*scsc*) described in Algorithm 1. When the update iteration terminates, we row-size concatenate the latent feature matrices $U^{(t)}$ of three views, including friendship, common friend and topic. Then, the concatenation is used as the final feature matrix, on which standard K-means is performed to find clusters. We chose these views as dominant views not only because they are generally denser (hence more complete), but also because they have demonstrated better discriminative information in our experiments. It should be noted, however, that although the interaction views are not directly used in final clustering, their information has already been transferred to the dominant views through the multi-view algorithms.

For comparison, we examine the performance of the following three clustering algorithms.

SCAN[54]: This is a popular algorithm designed for clustering nodes in a general network based solely on its structural information, which is typically taken as the friendship view of the network. Thus in experiment, we apply SCAN on the friendship view for finding circles. All its parameters are set as default.

Spectral Clustering (*sc*): this algorithm independently performs spectral clustering on the three dominant views for extracting their latent feature matrices $U^{(t)}$. Then, it concatenates three $U^{(t)}$'s in a row-size manner to form the final latent feature matrix, on which K-means is performed.

Co-trained Spectral Clustering (*csc*) [25]: this is the algorithm revisited in section 4.1. In experiment, we first apply it on six views to extract their latent feature matrices; similar to *cs*, those of the three dominant views are then concatenated to form the final feature matrix and K-means is performed on it to find circles.

It should be mentioned that, in experiments we observed similar trends of all approaches when varying the number of clusters k from 3 to 10. Thus we fix $k = 5$ for all approaches in reporting their final results (except SCAN that automatically determines this value).

5.3 Evaluation 1: Cluster Compactness

5.3.1 Evaluation Metric

Evaluating the clustering quality is challenging in our problem since neither the ground truth or feature matrix is available. This precludes the use of most standard external metrics such as random index and F-measure, and internal metrics such as Davies-Bouldin index and Dunn index. To address the problem, we present a new metric *total similarity ratio*, which requires only similarity

⁶If the maximum entry is zero, no normalization is performed. Also note normalization may slight change the interpretation of the similarity matrices, but would ideally not affect the clustering results.

matrices as input. To be specific, we expect alters within a circle to have high similarities and alters in different circles to have low similarities. Taking spirit from the classic discriminant analysis (e.g. [4, Formula (4)]), our metric evaluates the ratio between these two types of similarities. Given the similarity matrices $\{K^{(t)}\}$ of T views and *one* final clustering result (independent to t) indicated by matrix C , the metric is defined as

$$\gamma = \frac{\sum_{t \in [T]} S_w^{(t)}}{\sum_{t \in [T]} S_b^{(t)}}, \quad (27)$$

where ⁷

$$S_w^{(t)} = \frac{\sum_{(i,j) \in [n]^2} K_{ij}^{(t)} \cdot 1\{C_{ij} > 0\}}{\sum_{(i,j) \in [n]^2} 1\{C_{ij} > 0\}} \quad (28)$$

and

$$S_b^{(t)} = \frac{\sum_{(i,j) \in [n]^2} K_{ij}^{(t)} \cdot 1\{C_{ij} < 0\}}{\sum_{(i,j) \in [n]^2} 1\{C_{ij} < 0\}}. \quad (29)$$

The ratio can be interpreted as follows: $S_w^{(t)}$ estimates (for view t) the average similarity between alters that are assigned to the same cluster, which we call the *within-circle similarity*, while $S_b^{(t)}$ estimates the average similarity between alters assigned to different clusters, which we call the *between-circle similarity*. Then the ratio compares (over all views) the total within-circle similarity with the total between-circle similarity. It should be mentioned there are other ways to define the ratio such as $\sum_{t \in [T]} S_w^{(t)} / S_b^{(t)}$. We chose this one for its simplicity and stable performance revealed in experiments.

It is easy to extend metric (27) for evaluating clustering results on a single view t . Define the *similarity ratio* as:

$$\gamma^{(t)} = S_w^{(t)} / (S_b^{(t)} + \delta), \quad (30)$$

where $\delta > 0$ is a small constant in case $S_b^{(t)} = 0$, which occurred often if view t is very sparse.

5.3.2 Results and Discussions

To have a quick perception of the performance, we first examine the performance of *sc*, *csc* and the proposed *scsc* on one ego-net. The ego-net contains 386 alters and is described by the six views introduced in sections 3.2 and 5.1. We iterated both *csc* and *scsc* for 20 rounds of update and report their similarity ratios on each view in Figure 2. From the figure, we observe a general trend that the baseline method *csc* improves as more iterations are done. This coincides with the spirit of co-trained style learning algorithms. However, its convergence rate is relatively slow (as compared with *scsc*) and its improvements over the single-view spectral clustering are not significant on the views of topic and reply and are little on the views of friendship and co-reply. As explained before, these may be

⁷Define notation $[n]^2 = [n] \times [n]$.

due to the ignorance of *csc* on the possible incompleteness of the (sparse) views of the ego-net. On the other hand, *scsc* efficiently and significantly improves over single-view clustering in merely one or two iterations, and performs consistently better than the standard *csc*.

It is noted the methods are not consistently improving over the optimization iterations. Such fluctuation may be tied to multiple possible reasons: the standard K-means clustering on each view is sensitive to the choice of initial points (which may be alleviated by using the average result over multiple runs of K-means); the clustering results on very sparse (and potentially incomplete) views may not be very accurate; these not so accurate results are transferred to other views and mis-refine their similarity matrices (thus the fluctuation is more obvious for *csc*); the joint optimization problem is not convex; the learning model is still complex and subject to overfitting (thus the performance of both *csc* and *scsc* seem to decrease from the 19 iteration). Nevertheless, the general trend we observe is *scsc* converges faster and gives higher similarity ratio than *csc* on each view.

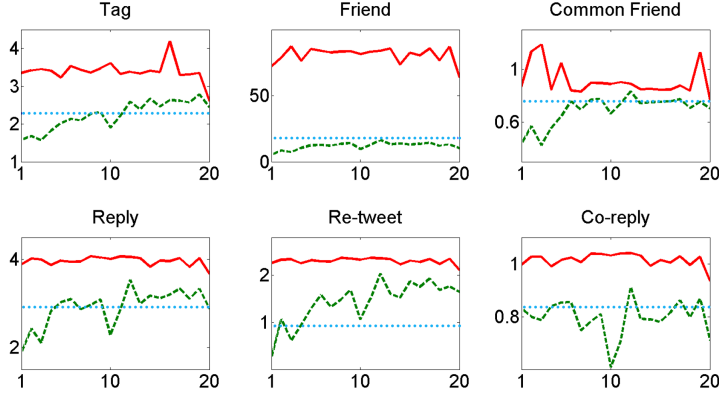


Figure 2: Similarity Ratios on Six Views. In each figure, the y-axis is the similarity ratio defined in (30) and x-axis is the number of update iterations. The blue dotted line represents the performance of single view spectral clustering, the green dash curve represents *csc* and the red solid curve represents the proposed *scsc* method.

Second, we examine the sizes of output clusters obtained on an ego-net containing 102 alters. For *csc* and *scsc*, we iteratively update their algorithms for 20 rounds and report the cluster sizes at their best performed step (i.e. when they achieve the highest similarity ratios over the 20 iterations). Table 1 summarizes the size of each cluster obtained by each method. From the table, it appears *csc* encourages more balanced clusters, while both *sc* and *scsc* output one big cluster. This may be because *csc* enforces stronger consistency across views, so that the sparser views manage to let the denser (dominant) views to ‘break down’ the inherent big clusters. It should be pointed out that, in practice imbalance clusters make sense in many situations. For instance, a family circle is usually much smaller than a friend circle.

Next, we evaluate the performance of *cs*, *csc* and *scsc* on 92 crawled ego-nets. The total similarity ratio of each method on each ego-net is shown in Figure 3.

Table 1: Sizes of the detected circles. *std* is the standard deviation over circles.

Cluster	1	2	3	4	5	std
<i>SC</i>	8	12	13	25	44	14.6
<i>CSC</i>	16	17	20	24	25	4.04
<i>SCSC</i>	10	10	13	15	54	18.9

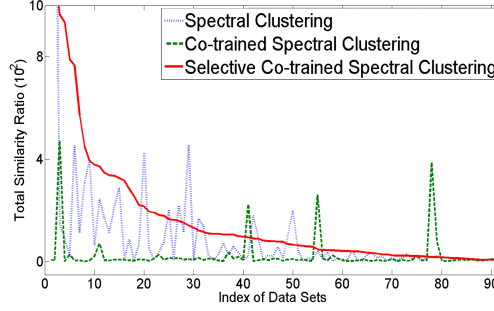


Figure 3: Total Similarity Ratio of all data sets. Each data set corresponds to one multi-view ego-net.

From the figure, we observe *scsc* outperforms both *sc* and *csc*, and that standard *csc* performs the worst. This coincides with our observations in Figure 2 and earlier discussions on the limitation of *csc*: it blindly transfers information from a possibly incomplete view to other views, which may mislead their clustering performance. The total similarity ratios averaged over all ego-nets are: 108.8 for *sc*, 24.8 for *csc* and 187.4 for *scsc*.

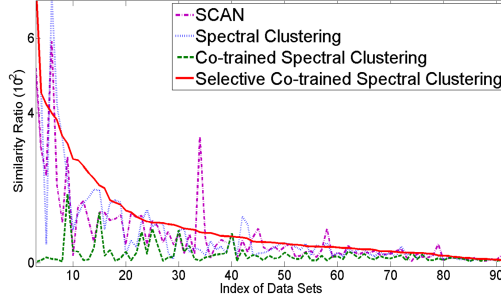


Figure 4: Similarity Ratio on the friend view of all data sets. Each data set corresponds to one multi-view ego-net.

Finally, we compare all methods on the ego-nets. In particular, we evaluate the performance of SCAN [54], which was designed for clustering based specifically on the friendship view. Since SCAN [54] removes *outliers* and report clustering results only on a set of confident alters, for fairness we performed and evaluated the rest methods on the same confident set only. The results are shown in Figure 4. Similar observations are found and the average total similarity ratios are 71.9 for SCAN, 79.5 for *cs*, 20.9 for *csc* and 100.6 for *scsc*. The results suggest that neither single view ego-net nor complete view transfer suffices to give a high quality clustering.

5.4 Evaluation 2: Quality of Boundary Alters

Our second investigation is to manually evaluate the qualities of the detected circles for the *scsc* method. Since it is too expensive in both time and labor to examine all alters, we focus on *boundary alters* – those are farthest from the centers of their assigned circles, since they are more likely to be mis-assigned. The general idea is to ask a human evaluator to decide (without any prior information) whether a boundary alter should be assigned to one of the following two circles: 1) the *assigned circle*, which this alter is assigned to by the clustering method; 2) the *neighbor circle*, which this alter is most similar to yet not assigned to. The neighbor circle of an alter is identified as the non-assigned circle (in the same ego-net as that alter) whose members have the smallest distance to that alter on average.

To be specific, our evaluation protocol is as follows. First, 60 boundary alters are randomly selected from the ego-nets. For each boundary alter, we first randomly select 10 other alters (in its same ego-net), with 5 from its assigned circle and 5 from its neighbor circle; then, the profiles and posts of these ten alters are presented to a human evaluator, who is then asked to score from 1 to 5 whether he/she agrees the boundary alter should be assigned to the same circle as every one of the selected alters – 1 for strongly disagree, 2 for somewhat disagree, 3 for neutral, 4 for somewhat agree and 5 for strongly agree; finally, two average scores are computed, with one averaged over the 5 alters from the assigned circle and the other averaged over the 5 alters from the neighbor circle. Five evaluators participated in the scoring, and none of them had prior information about the clustering result.

We summarize these two scores for each boundary alter, and found their averages (over 60 boundary alters) are 2.63 for alters from the assigned circles and 2.52 for alters from the neighbor circles. The implication of this result is twofold. On one hand, the difference between these two scores are not very significant. This may imply most boundary alters are indeed people who are likely to participate in multiple circles. On the other hand, the score is higher for alters from the same circle. This implies *scsc* could properly assign the boundary alters into the circles to which they have tighter connections. This could be considered as one way of converting overlapping circles into non-overlapping circles.

5.5 Evaluation 3: Keyword Extraction for Clusters

For better interpreting the results, we inspect the topics of the detected circles by finding their most relevant tags. The search contains two parts: finding *relevant* tags that are related to the content of each circle and finding *representative* tags that are discriminative across circles.

To find relevant tags, consider an ego-net. Recall we have applied the online annotation tool TagMe to extract for each alter a set of relevant tags. Let t denote an arbitrary tag, T_i denote the set of tags relevant to alter i and \mathcal{S} denote an arbitrary circle, which is the index set of alters assigned to that circle. The relevance between t and \mathcal{S} is computed as

$$\Pr\{t|\mathcal{S}\} = \frac{\sum_{i \in \mathcal{S}} \tilde{f}(i, t)}{|\mathcal{S}|}, \quad (31)$$

Table 2: Representative tags for detected circles in an ego-net.

Circle	Representative Tags
\mathcal{S}_1	Human, Sleep
\mathcal{S}_2	Valentine’s Day, Dance, Sport
\mathcal{S}_3	Ireland, Beer, Coffee
\mathcal{S}_4	Social media, Health, Cancer
\mathcal{S}_5	Yahoo!, WHATS’On (Software), Android

where

$$\tilde{tf}(i, t) = \frac{tf(i, t)}{\max\{tf(i, t) | t \in T_i\}}. \quad (32)$$

and $tf(i, t)$ is the frequency of tag t appeared in the content of alter i , and function \max returns the largest tag frequency in the alter’s content. The larger the probability is, the more relevant tag t is considered to the circle \mathcal{S} .

To find representative tags, we use a KL-divergence style measurement. Let \mathcal{S}_i be the set of circle indexed by $i \in \mathcal{I}_{\mathcal{S}}$. For each tag t , let its normalized relevance to circle \mathcal{S}_i be

$$P_t(i) = \frac{\Pr\{t | \mathcal{S}_i\}}{\sum_{i \in \mathcal{I}_{\mathcal{S}}} \Pr\{t | \mathcal{S}_i\}}, \quad (33)$$

and the un-representative relevance to circle \mathcal{S}_i be

$$Q_t(i) = \frac{1}{|\mathcal{I}_{\mathcal{S}}|}. \quad (34)$$

Note both P_t and Q_t can be interpreted as probability mass. Then, the ‘representativeness’ of tag t is evaluated by

$$D_{KL}(t) = \sum_{i \in \mathcal{I}_{\mathcal{S}}} \left(P_t(i) \ln \frac{P_t(i)}{Q_t(i)} \right). \quad (35)$$

Formula (35) can be interpreted as follows: the probability Q_t gives a tag that distributed even across all circles and thus not representative for any circle; the larger KL-distance between P_t and Q_t , the more unevenly is t distributed across circles and thus this tag is more representative for some circles.

In summary, we first apply (35) over tags obtained for all alters to find the most representative ones; then, among these tags we apply (31) for each circle to find its three most relevant tags. Our finding are showed in Table 2.

From the table, we see different circles focus on different topics. For instance, circle 2 is more concerned about entertainment, circle 4 seems to be more interested in health care and circle 5 favors technology. We manually examined the posts of these circles and had consistent finding of the above results. This suggests the detected circles could be pretty interpretable from the topic viewpoint.

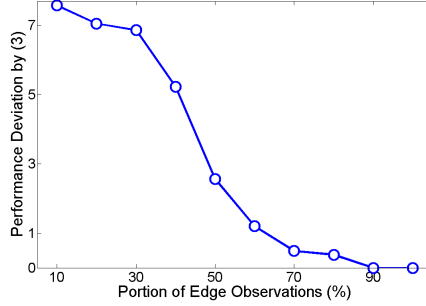


Figure 5: Performance deviation on graph K and its incomplete observation \tilde{K} based on metric (3).

5.6 Evaluation 4: Effect of Graph Sparsity

A direct and important implication of Proposition 1 is as the graph becomes more observed, the performance deviation of standard clustering method would decrease. Since in reality it is impossible to know whether a social network has been fully observed, we present simulations in this section to verify this implication.

Consider a set of 200 nodes partitioned into k_* groups, each containing $\lfloor 200/k_* \rfloor$ nodes. (The last group also contains the residual nodes.) We construct a binary graph in the follow way: build an edge between each pair of nodes, with probability p if they are from the same group and with probability $1 - p$ otherwise. The resulted graph is considered as the underlying complete graph. Note this graph can be fully characterized by its adjacent matrix $K \in \mathbb{R}^{200 \times 200}$ such that $K_{ij}=1$ with probability p if nodes i and j are from the same group and with probability $1-p$ otherwise.

To simulate partial observations of the graph, we randomly hide a portion of its edges. This corresponds to flipping a portion of 1's in K into 0's. Let δ be the portion of un-flipped 1's and \tilde{K} be the resulted adjacent matrix. Then, we apply the standard spectral clustering (e.g. [39]) on both K and \tilde{K} and evaluate the difference of their performance based on metric (3). To minimize the performance variation of the K-means clustering method (induced from its selection of initial cluster centers), we fix one node for each group to form the initial centers.

In Figure 5, we show the performance deviation as the observations increase with $k_*=5$. It is clear the deviation decreases as more observations are obtained, which is consistent with the implication of our bound.

Second, we show the performance deviation under different choice of detected clusters (i.e. parameter k in (4)) in Figure 6. For each choice, the initial cluster centers are chosen by a standard 'cluster' setting in Matlab (i.e. 10% of the nodes are randomly sampled to perform clustering first, and centers of the resulted clusters are used as the initial centers for the whole data set). From the figure, it is clear that smaller choice of k suffers smaller performance deviation. This is consistent with the implication of our theoretical bound in (4), which decreases as k decreases.

Finally, we examine the impact of coefficient σ_1/σ_n . Fix $k_*=5$, $k=5$ and

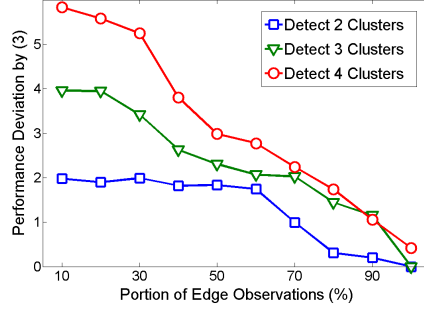


Figure 6: Performance deviation on graph K and its incomplete observation \tilde{K} based on metric (3).

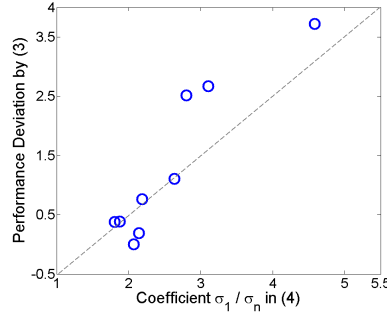


Figure 7: Performance deviation on graph K and its incomplete observation \tilde{K} based on metric (3).

$\delta=30\%$ so that we have 5 underlying groups of nodes for constructing the graph. The probabilities of generating edges between node pairs from the last four groups and from different groups remain the same; for node pairs from the first group, we generate edges between them with probability p' varying from 0.1 to 0.9 (with step length fixed as 0.1). Note different choices of p' generates different graphs. For each choice of p' , we apply spectral clustering on both its induced K and \tilde{K} , and evaluate the performance deviation. Meanwhile, we also record the coefficient σ_1/σ_n induced from K . Finally, the deviation-coefficient pair of each p' is plotted as a point in Figure 7.

From the figure we have three observations. First, in general a larger coefficient σ_1/σ_n corresponds to larger performance deviation. This is consistent with the implication of our bound. Second, the relation between the coefficient and deviation is roughly linear, which also coincides with our result. It is noted, however, such relation does not cross the origin as suggested by the bound; instead, it is biased by a nearly constant factor. We believe such bias is reasonable and should be largely induced from the approximation error of spectral clustering. (Recall we have abstracted away by the free-approximation assumption.) It is for this reason we do not claim our bound tight. However, its multiple implications are verified from the simulations and may provide useful insights for algorithm designs.

6 Related Work

6.1 Social Circle Clustering

Identifying social circles from a user’s online social networks is important for the individual to exert appropriate access control on information sharing [45, 12]. However, manually managing groups on social network sites might present a burden for users, which triggered the idea on using automatic sociocentric network clustering algorithms. The feasibility of this idea has been demonstrated in the findings from [17, 22].

Sociocentric network clustering, which is usually referred to as community detection, aims to divide people into groups within which they are more similar[1] and have more connections[38] or relationships. Unlike traditional personal network studies, which focus on attribute-based data such as age, sex [35], most of graph-based methods in community detection[16], which include traditional methods like graph partitioning[24] and hierarchical clustering[38], modern methods through maximization of a likelihood like [37], and more recent methods based on matrix factorization like [59], only consider topological structure and linkage information. But there is a trend in recent research based on graphs which combined link information and content or attribute information[56, 40] or interaction information between individuals[62].

Compared with graph-based methods, another class of approaches attach greater importance to content or link context information. [9, 31, 60, 61] use state-of-the-art method like topic modeling to take full advantage of semantic information, such as email, tweet messages, and documents, in detecting communities from a social network. [51] proposed a method to find like-minded people who share more semantically relevant tags.

A recent research more related to ours is [41]. It proposed generative Bayesian models to utilize not only topics and social graph topology but also nature of user interactions to discover latent communities in social graphs. The difference between their work and ours is that we also used tag annotation method to analyze content information generated by users, which concerns the understanding of the information and is more meaningful in finding similar topics.

Based on privacy concerns and automatic social circle detection, [32] developed a model to discover social circles by using both network structure and user profile information; [46] proposed an approach based on apriori algorithm to identify hidden groups by dynamically detecting grouping criteria, i.e. certain combinations of properties of a user’s contacts, such as relationship, location, hobbies, age, privacy, etc. The difficulty in utilizing this kind of methods is that automatically collecting attributes of users through online social network is a nontrivial task although traditional personal network studies can collect these information through interviews more easily.

6.2 Multi-View Spectral Clustering

Multi-view spectral clustering is a framework that effectively combines information from multiple sources under the view consistency idea. It has demonstrated superior performance in many applications such as document categorization [5], digit classification [25, 27] and image annotation [50]. However, to our knowledge this framework has not been applied for detecting social circles, and our

work is the first effort in this direction.

In this paper, we base our analysis on the co-trained spectral clustering algorithm [25] for its direct use of the similarity matrices as input, which is needed in our problem setting. During investigation, we noticed a limitation of this algorithm, i.e. it assumes all views are complete and equally transfer information across views. In our problem, however, some views are very sparse and potentially incomplete. In this case, equally transferring information among different views may mislead clustering and hurt the performance. We present theoretical analysis on the performance degeneration and propose a modification of the co-trained spectral clustering algorithm. In experiment we show the modified algorithm indeed improves the performance.

6.3 Clustering on Incomplete Graph

Clustering on incomplete graphs is not a new topic. See studies in [10, 48, 42, 28] for example. Most of these works provided only algorithmic solutions and a few theoretical studies assumed prior knowledge on which part of the graph is missing. However, none of them address our concern on the performance deviation between clustering a graph and its incomplete observation.

A work more related to ours is [23], which analyzes how much the spectral clustering solution on a *complete* graph may deviate from the optimal normalized cut solution. Our analysis focuses on a fundamentally different problem, i.e. how much would two spectral clustering solutions deviate, with one based on a complete graph and the other based on its incomplete observation. Technically, we use the same evaluation metric as [23] and borrow some of its results, while additionally introducing perturbation theories to incorporate the incomplete observation.

Another related work is [21], which analyzes the effect of graph perturbation on the performance of spectral clustering. We study the same research question, but our analysis is fundamentally different from theirs in at least three aspects. First, the problem settings are different: they study only bi-partitioning based on the second principal eigen-vector, while we study multi-partitioning based on the k learning eigen-vectors. Second, the evaluation metrics are different: their metric does not consider the cluster sizes while ours does. Third, the proving techniques are different: they use a water-filling argument whereas we largely rely on the fundamental properties of Loewner partial orders; we also borrow a latest perturbation result from [57] and some results in [23].

7 Discussions

7.1 Non-Overlapping vs. Overlapping Circles

Two settings of circle detection have been investigated in the literature, i.e. detecting overlapping circles and detecting non-overlapping circles. The former assigns each alter to at most one circle (e.g. [36, 18]), while the latter allows each alter to be assigned to more than one circle (e.g. [34]). In this paper, we focus on the non-overlapping setting. One reason is it is a more fundamental setting that can be admitted by the overlapping setting. For instance, two overlapping circles (each represented by an index set of their contained alters) \mathcal{S}_1 and \mathcal{S}_2

admit three non-overlapping counterparts, that is, $\mathcal{S}_1 \cap \mathcal{S}_2$, $\mathcal{S}_1 \setminus \mathcal{S}_2$ and $\mathcal{S}_2 \setminus \mathcal{S}_1$; in addition, if a circle \mathcal{S}_1 is contained in another circle \mathcal{S}_2 (i.e. $\mathcal{S}_1 \subseteq \mathcal{S}_2$), then together they admit two disjoint counterparts \mathcal{S}_1 and $\mathcal{S}_2 \setminus \mathcal{S}_1$.

Another reason to focus on non-overlapping setting is from the privacy protection perspective, which is the main application that motivates our study. A major approach to protect privacy on social network is to draw information boundaries between circles so that an ego’s post is spread only within a designated circle. However, in an overlapping setting, an alter assigned to multiple circles may easily break such boundary. Imagine a message sent to a designated circle. If an alter in this circle is also assigned to another non-designated circle, then his actions on the message (such as ‘like’ or ‘retweet’) may reveal it to alters in the non-designated circles, violating the privacy concern of the ego.

We do admit, however, in reality there may be alters who have tight connections to multiple circles, and in experiment they seem to increase the challenge of clustering. Through manual examination of the detected disjoint circles, we have several observations: 1) such a ‘multi-tied’ alter is usually assigned to a single circle whose members have stronger connection to him/her; 2) when there are many alters connecting to two circles and these alters strongly connect to each other, we may end up identifying three circles; 3) conditioned on the second case, when many alters are simultaneously connecting to multiple circles, we may also end up finding a big circle that merges these circles.

In the third case, one may ask whether the combination of circles would break the information boundaries built for privacy protection. We view this issue from three aspects. First, the information boundaries are those subjectively *confirmed* by the ego, and the purpose of privacy protection is to prevent information from crossing the boundary. Therefore, once a set of circles are detected and confirmed by the ego, it is no longer a concern whether some large circles in the set may ‘break the boundary’. For instance, in Table 2 the second circle contains both Valentine’s Day and Sport. By assuming they are irrelevant, it looks like this circle has combined two possibly overlapping circles, one focused on topic Valentine’s Day and the other focused on Sport. Nevertheless, if the ego accepts this circle (implying he is okay with sending message to people interested in both topics), this circle does not break any information boundary. Second, we admit the combination of circles may provide the ego with a coarser information boundary, since a large circle may contain a mixture of diverse topics. If the ego wish to further separate these topics, a possible remedy is to take this circle as an ‘ego-net’ and detect social circles within it again. In this case, we may employ hierarchical clustering as the core technique. Finally, it should be recalled our results are based on the information from six views. Even if two small circles tend to be combined in the topic view, they may still remain separate if their connections are really weak in other views. (Otherwise, it makes even more sense to combine them.)

7.2 Applications of Social Circles

A potential application of social circle is to draw information boundary between different circles, so that a message could be delivered only to designated circles (e.g. [46, 47]). Note the final social circle construction does not have to be entirely automatic, and the ego may manually modify the detected groups. In this case, circle detection still significantly reduces the effort of human labeling.

Another issue is the information boundaries may not be completely secure if the social networking sites allows breaches in privacy protection (e.g. alters could ‘re-share’ their received private posts). These are, however, beyond the scope of the paper.

The discovered social circles could also be used to improve the efficiency of ad delivery, targeted advertising, and opinion mining in social groups. (See [33] for more discussions.) Social circles could also be used to study users’ socialization behavior and social network information flow. When the temporal information of data is available, our methods may be further extended to detect circles in evolving ego-nets. (See a latest progress on dynamic social network analysis in [52] for instance.) In addition, when information of the ego-net is available from other domains (e.g. [30, 53]), it is possible to further improve our work by considering cross-domain cross-view social circle detection.

8 Conclusion

In this paper, we propose to automatically detect social circles of an ego-net based on its multi-view network structure. We construct multi-view ego-nets from Twitter and apply multi-view spectral clustering methods to detect circles. In experiment we show superior performance of multi-view clustering methods, and the benefit of treating sparse networks as incomplete ones. We discuss the harm of ignoring such incompleteness in both theory and simulation.

References

- [1] L. A. Adamic and E. Adar. Friends and neighbors on the web. *Social Networks*, 25:211–230, 2003.
- [2] F. R. Bach and M. I. Jordan. Learning spectral clustering. *Computer Science*, 2003.
- [3] M.-F. Balcan, A. Blum, and K. Yang. Co-training and expansion: Towards bridging theory and practice. In *NIPS*, 2004.
- [4] P. N. Belhumeur, J. P. Hespanha, and D. J. Kriegman. Eigenfaces vs. fisherfaces: Recognition using class specific linear projection. *Pattern Analysis and Machine Intelligence, IEEE Transactions on*, 19(7):711–720, 1997.
- [5] S. Bickel and T. Scheffer. Multi-view clustering. In *ICDM*, 2004.
- [6] A. Blum and T. Mitchell. Combining labeled and unlabeled data with co-training. In *COLT*.
- [7] T. Chakraborty, S. Patranabis, P. Goyal, and A. Mukherjee. On the formation of circles in co-authorship networks. In *SIGKDD*, 2015.
- [8] H.-W. Chang, D. Lee, M. Eltaher, and J. Lee. @phillies tweeting from philly? predicting twitter user locations with spatial word usage. In *ASONAM*, 2012.
- [9] J. Chang, J. Boyd-Graber, and D. M. Blei. Connections between the lines: augmenting social networks with text. In *SIGKDD*, 2009.

- [10] Y. Chen, A. Jalali, S. Sanghavi, and H. Xu. Clustering partially observed graphs via convex optimization. *The Journal of Machine Learning Research*, 15(1):2213–2238, 2014.
- [11] Z. Cheng, J. Caverlee, and K. Lee. You are where you tweet: a content-based approach to geo-locating twitter users. In *Proceedings of the 19th ACM international conference on Information and knowledge management*, pages 759–768. ACM, 2010.
- [12] d. m. boyd and N. B. Ellison. Social network sites: definition, history and scholarship. *Journal of Computer-Mediated Communication*, 13:210–230, 2008.
- [13] C. Davis and W. M. Kahan. The rotation of eigenvectors by a perturbation. iii. *Journal on Numerical Analysis*, 1970.
- [14] K. Dykstra, J. Lijffijt, and A. Gionis. Covering the egonet: A crowdsourcing approach to social circle discovery on twitter. In *Proceedings of the 9th International AAAI Conference on Web and Social Media*. AAAI Publications, 2015.
- [15] P. Ferragina and U. Scaiella. Fast and accurate annotation of short texts with wikipedia pages. *Software, IEEE*, 29(1):70–75, 2012.
- [16] S. Fortunato. Community detection in graphs. *Physics Reports*, 486:75–174, 2010.
- [17] E. Gilbert and K. Karahalios. Predicting tie strength with social media. *CHI’09*, pages 211–220, 2009.
- [18] M. Girvan and M. E. Newman. Community structure in social and biological networks. *Proceedings of the national academy of sciences*, 99(12):7821–7826, 2002.
- [19] G. H. Golub and C. F. Van Loan. *Matrix computations*. 2012.
- [20] R. A. Horn and C. R. Johnson. *Matrix analysis*. Cambridge university press, 2012.
- [21] L. Huang, D. Yan, N. Taft, and M. I. Jordan. Spectral clustering with perturbed data. In *NIPS*, 2009.
- [22] S. Jones and E. O’Neill. Feasibility of structural network clustering for group-based privacy control in social networks. *SUPS*, 2010.
- [23] F. Jordan and F. Bach. Learning spectral clustering. *NIPS*, 2004.
- [24] B. W. Kernighan and S. Lin. An efficient heuristic procedure for partitioning graphs. *The Bell System Technical Journal*, 1970.
- [25] A. Kumar and H. D. Iii. A co-training approach for multi-view spectral clustering. In *ICML*, 2011.
- [26] A. Kumar, P. Rai, and H. Daume. Co-regularized multi-view spectral clustering. In *NIPS*, 2011.

- [27] A. Kumar, P. Rai, and H. D. Iii. Co-regularized multi-view spectral clustering. In *NIPS*, 2011.
- [28] S.-Y. Li, Y. Jiang, and Z.-H. Zhou. Partial multi-view clustering. In *AAAI*, 2014.
- [29] W. Li, P. Serdyukov, A. P. de Vries, C. Eickhoff, and M. Larson. The where in the tweet. In *CIKM*, 2011.
- [30] S. Liu, S. Wang, and F. Zhu. Structured learning from heterogeneous behavior for social identity linkage. *Knowledge and Data Engineering, IEEE Transactions on*, 27(7):2005–2019, 2015.
- [31] Y. Liu, A. N. Mizil, and W. Gryc. Topic-link lda: Joint models of topic and author community. *ICML '09*, 382:665–672, 2009.
- [32] J. McAuley and J. Leskovec. Discovering social circles in ego networks. *TKDD'13*, 2012.
- [33] J. McAuley and J. Leskovec. Discovering social circles in ego networks. *ACM Transactions on Knowledge Discovery from Data (TKDD)*, 8(1):4, 2014.
- [34] J. J. McAuley and J. Leskovec. Learning to discover social circles in ego networks. In *NIPS*, 2012.
- [35] C. McCarty. Structure in personal networks. *Journal of Social Structure*, 3, 2002.
- [36] M. E. Newman. Modularity and community structure in networks. *Proceedings of the national academy of sciences*, 103(23):8577–8582, 2006.
- [37] M. E. J. Newman and E. A. Leicht. Mixture models and exploratory analysis in networks. *Proc Natl Acad Sci USA*, 104, 2007.
- [38] M. E. J. Newman and M. Girvan. Finding and evaluating community structure in networks. *Rhys. Reve. E*, 69:026113, Feb 2004.
- [39] A. Y. Ng, M. I. Jordan, Y. Weiss, et al. On spectral clustering: Analysis and an algorithm. *NIPS*, 2002.
- [40] Y. Ruan, D. Fuhry, and S. Parthasarathy. Efficient community detection in large networks using content and links. *WWW*, 2013.
- [41] M. Sachan, D. Contractor, T. A. Faruque, and L. V. Subramaniam. Using content and interactions for discovering communities in social networks. *WWW'12*, pages 331–340, April 2012.
- [42] W. Shao, X. Shi, and P. S. Yu. Clustering on multiple incomplete datasets via collective kernel learning. In *ICDM. IEEE*, 2013.
- [43] J. Shi and J. Malik. Normalized cuts and image segmentation. *Pattern Analysis and Machine Intelligence, IEEE Transactions on*, 22(8):888–905, 2000.

- [44] P. Shi, H. Xu, and Y. Chen. Using contextual integrity to examine interpersonal information boundary on social network sites. In *CHI*.
- [45] M. M. Skeels and J. Grudin. When social networks cross boundaries: a case study of workplace use of facebook and linkedin. *GROUP'09*, May 2009.
- [46] A. Squicciarini, S. Karumanchi, D. Lin, and N. DeSisto. Identifying hidden social circles for advanced privacy configuration. *Computers & Security*, 2013.
- [47] A. Squicciarini, D. Lin, S. Karumanchi, and N. DeSisto. Automatic social group organization and privacy management. In *CollaborateCom*, 2012.
- [48] R. K. Vinayak, S. Oymak, and B. Hassibi. Graph clustering with missing data: Convex algorithms and analysis. In *NIPS*, 2014.
- [49] U. Von Luxburg. A tutorial on spectral clustering. *Statistics and computing*, 17(4):395–416, 2007.
- [50] H. Wang, F. Nie, and H. Huang. Multi-view clustering and feature learning via structured sparsity. 2013.
- [51] X. Wang, H. Liu, and W. Fan. Connecting users with similar interests via tag network inference. *CIKM*, 2011.
- [52] B. Wu, T. Mei, W.-H. Cheng, and Y. Zhang. Unfolding temporal dynamics: Predicting social media popularity using multi-scale temporal decomposition. In *NIPS*, 2004.
- [53] S.-H. Wu, H.-H. Chien, K.-h. Lin, and P. Yu. Learning the consistent behavior of common users for target node prediction across social networks. In *ICML*, 2014.
- [54] X. Xu, N. Yuruk, Z. Feng, and T. A. Schweiger. Scan: a structural clustering algorithm for networks. In *SIGKDD*. ACM, 2007.
- [55] J. Yang, J. McAuley, and J. Leskovec. Community detection in networks with node attributes. In *ICDM*. IEEE, 2013.
- [56] T. Yang, R. Jin, Y. Chi, and S. Zhu. Combining link and content for community detection: a discriminative approach. *KDD*, 2009.
- [57] Y. Yu, T. Wang, and R. J. Samworth. A useful variant of the davis–kahan theorem for statisticians. *Biometrika*, 102(2):315–323, 2015.
- [58] H. Zha, X. He, C. Ding, M. Gu, and H. D. Simon. Spectral relaxation for k-means clustering. In *NIPS*, 2001.
- [59] Y. Zhang and D.-Y. Yeung. Overlapping community detection via bounded nonnegative matrix tri-factorization. *KDD*, August 2012.
- [60] D. Zhou, E. Manavoglu, J. Li, C. L. Giles, and H. Zha. Probabilistic models for discovering e-communities. *WWW*, 2006.
- [61] W. Zhou, H. Jin, and Y. Liu. Community discovery and profiling with social messages. *KDD'12*, pages 388–396, August 2012.

- [62] Y. Zhou and L. Liu. Social influence based clustering of heterogeneous. *KDD'13*, August 2013.